

Interaction-enhanced quantum to classical crossover temperature in a Luttinger liquid

Yen-Wen Lu and Michael Mulligan

Department of Physics and Astronomy,

University of California, Riverside, California 92511, USA

(Dated: July 9, 2025)

We study electrical and thermal transport in a one-dimensional Luttinger liquid coupled to a three-dimensional acoustic phonon in both the “clean” (umklapp scattering) and “dirty” (disorder scattering) limits using the memory matrix formalism. By explicitly incorporating the Debye cutoff on phonon frequencies, we consider the low and high temperature transport regimes. We find the crossover temperature separating these two regimes to be interaction-dependent, with repulsive interactions increasing the crossover temperature by at most an order of magnitude. This provides an illustration for how interactions can enhance the low-temperature scattering regime in an interacting Fermi system.

CONTENTS

I. Introduction	1
II. Model	2
A. Decoupled Fixed Point	2
B. Current Relaxation	4
III. Transport at low and high temperatures	5
A. Memory Matrix	5
B. Umklapp scattering	6
C. Regularizing the free fermion point	10
D. Disorder scattering	10
IV. Crossover temperature	11
V. Conclusion	14
Acknowledgments	15
A. Static Susceptibilities	16
B. Evaluation of $F_{m,\mathcal{Q}}^i$	17
C. Disorder Scattering Memory Matrix Details	17
References	19

I. INTRODUCTION

An infamous property of strongly correlated electron systems—from cuprate and heavy-fermion superconductors to twisted bilayer graphene—is robust T -linear electrical resistivity over unusually wide temperature ranges [1–4]. There are (at least) two features to distinguish here: the first is the T -linear exponent; the second is the multiple orders of magnitude in temperature over which this exponent persists without apparent change. (“Robust” refers to the appearance of this behavior in a variety of disparate materials, seemingly ruling out an explanation that invokes fine-tuning.) Linear behavior at low temperatures can occur in non-Fermi liquids [5–7]—although there can be more conventional instances, e.g., in doped semiconductors [8] or dilute metals [9] over limited temperature ranges—and may reflect a “universal” Planckian scattering rate $\tau^{-1} \propto k_B T / \hbar$ [4, 10]. This Planckian timescale represents a possible bound on dissipation in quantum systems.

In this paper, we are *not* interested in the T -linear exponent. Rather, we are interested in the second feature: the persistence of a fixed exponent across a large temperature range. This phenomenon is particularly puzzling given that different microscopic dissipation mechanisms are expected to govern transport at different temperatures. Electron-phonon scattering provides the canonical example: In conventional metals, it produces T^5 electrical resistivity at low temperatures and T -linear electrical resistivity at sufficiently high temperatures [11]. If electron-phonon scattering is also present in strongly correlated electron systems, why does the resistivity slope in the “classical” high-temperature regime coincide with that at lower temperatures where quantum effects should prevail?

We propose that electron-electron interactions can modify the crossover temperature between quantum and classical transport regimes. Specifically, strong correlations may enhance the crossover scale, effectively extending the quantum regime to higher temperatures where classical behavior would otherwise emerge. This mechanism could explain the persistence of non-Fermi liquid transport at elevated temperatures without invoking coincidental matching of scattering rates.

To test this proposal, we study transport in a one-dimensional Luttinger liquid coupled to a three-dimensional acoustic phonon, a system previously studied in [12]. We use bosonization to treat certain electron-electron interactions exactly and the memory matrix formalism to systematically compute transport coefficients across all temperatures. We calculate both electrical σ and thermal κ conductivities in clean (umklapp-dominated) and dirty (disorder-dominated) limits, explicitly incorporating the Debye cutoff on phonon frequencies. We assume a weak electron-phonon coupling and an arbitrarily strong, repulsive electron-electron interaction.

At low temperatures and in the clean limit, for example, we find $\sigma \propto T^{1-2K}$ and $\kappa \propto T^{2-2K}$. Here, $K \leq 1$ parameterizes the effective interaction strength: $K = 1$ at the free

fermion point, while $K < 1$ represents repulsive interactions. At sufficiently high temperatures, these exponents are increased by +2. Our central observation is that the crossover temperature $T_0(K)$ between the low and high temperature regimes is interaction-dependent. For strong repulsive interactions ($K \ll 1$), $T_0(K)$ can be enhanced by up to an order of magnitude relative to the non-interacting case.

The remainder of the paper is organized as follows. In §II we introduce our conventions for describing a Luttinger liquid coupled to phonons. In §III we calculate the electrical and thermal conductivities of our system at low and high temperatures: we first introduce the memory matrix formalism; then we calculate these conductivities in the clean and dirty limits. In §IV we extract the crossover temperature $T_0(K)$ between low and high temperature regimes and observe how electron-electron interactions can enhance this temperature. In §V we conclude. We provide the details of the calculations presented in the main text in a series of appendices.

II. MODEL

A. Decoupled Fixed Point

We consider a single channel of spinless fermions in one spatial dimension, with low-energy Hamiltonian:

$$H_{LL} = H_{\text{lin}} + H_{\text{int}}. \quad (\text{II.1})$$

The non-interacting Hamiltonian is

$$H_{\text{lin}} = -iv_F \int_x (\psi_R^\dagger \partial_x \psi_R - \psi_L^\dagger \partial_x \psi_L). \quad (\text{II.2})$$

Here, $\psi_{R/L}^\dagger$ creates a right/left-moving fermion with Fermi velocity v_F about the Fermi point $\pm k_F$; we abbreviate $\int_x \equiv \int dx$. The interacting Hamiltonian consists of two terms,

$$H_{\text{int}} = V_f + V_b, \quad (\text{II.3})$$

where the forward-scattering V_f and backward-scattering V_b terms,

$$V_f = \pi g_4 \int_x (\rho_R^2(x) + \rho_L^2(x)), \quad V_b = 2\pi g_2 \int_x \rho_R(x) \rho_L(x), \quad (\text{II.4})$$

and $\rho_{R/L}(x)$ is the number density operator for right/left-movers. Repulsive interactions have $g_2 > 0$.

The low-energy Hamiltonian can be treated exactly using bosonization [13]:

$$H_{LL} = \frac{v_e}{8\pi} \int dx \left(K(\pi\Pi)^2 + \frac{1}{K}(\partial_x\phi)^2 \right), \quad (\text{II.5})$$

where the canonical momentum $\Pi = (\partial_x \theta)/\pi$,

$$v_e = \sqrt{(v_F + g_4)^2 - g_2^2}, \quad K = \left[\frac{v_F + g_4 - g_2}{v_F + g_4 + g_2} \right]^{\frac{1}{2}}. \quad (\text{II.6})$$

Forward scattering g_4 can be absorbed into a redefinition of the Fermi velocity v_F . The Luttinger parameter $K < 1$ for repulsive interactions ($g_2 > 0$). Notice that the Luttinger velocity $v_e \rightarrow 0$ as $K \rightarrow 0$. We therefore require $K > 0$. The right/left-moving fermion operators are related to the Luttinger bosons (ϕ and θ) as

$$\psi_{R/L}(x) = \frac{1}{\sqrt{2\pi a}} e^{i(\pm\phi - \theta)}, \quad (\text{II.7})$$

where $\phi = (\varphi_L + \varphi_R)/2$ and $\theta = (\varphi_L - \varphi_R)/2$, with right/left-moving bosons $\varphi_{R/L}$; $a > 0$ is a short-distance cutoff.

Acoustic phonons have the Hamiltonian,

$$H_{ph} = \int \frac{d^3x}{2\pi} \left[(\pi P)^2 + \sum_{i=x,y,z} v_i^2 (\partial_i q)^2 \right]. \quad (\text{II.8})$$

Here P is the canonical momentum for the phonons with “coordinate” q and velocity v_i along direction $i \in \{x, y, z\}$. We denote $v_x = v_p$ and $v_y = v_z = v_\perp$, i.e., the phonon velocities parallel and perpendicular to the direction of propagation of the Luttinger bosons.

The decoupled fixed point Hamiltonian for the Luttinger boson + acoustic phonon system is

$$H_0 = H_{LL} + H_{ph}. \quad (\text{II.9})$$

This fixed point Hamiltonian has an infinite number of conserved quantities. We are interested in the “slowly-decaying” symmetries associated with translation invariance, charge (or fermion number) conservation, and energy conservation that are preserved when the Luttinger boson and acoustic phonon are coupled together. These symmetries have the following conserved currents: the momentum operator,

$$P_D = \int_x \Pi(\partial_x \phi) + \int d^3x P(\partial_x q), \quad (\text{II.10})$$

or, equivalently, the “momentum current” $J_D = -v_e^2 P_D$; the electrical current,

$$J_e = \frac{ev_e K}{4} \int_x \Pi; \quad (\text{II.11})$$

and the heat current,

$$J_T = -\frac{v_e^2}{4} \int_x \Pi(\partial_x \phi) - v_p^2 \int d^3x P(\partial_x q). \quad (\text{II.12})$$

B. Current Relaxation

The currents $\{J_D, J_e, J_T\}$ commute with H_0 in (II.9). Consequently, the decoupled fixed point has infinite conductivity. Finite conductivity requires current relaxation, i.e., we need to supplement H_0 with terms that do not commute with $\{J_D, J_e, J_T\}$.

We will study two different types of current relaxation mechanisms that couple the Luttinger boson and acoustic phonon: umklapp scattering,

$$H^U = \sum_{m \geq 1} H_m^U = - \sum_m \lambda_m^U \int_x \left[\frac{1}{a^m} e^{i\bar{k}_m x} e^{im\phi} \partial_x q + \text{h.c.} \right]; \quad (\text{II.13})$$

and disorder-mediated scattering,

$$H^{\text{dis}} = \sum_{m \geq 1} H_m^{\text{dis}} = \sum_m \lambda_m^{\text{dis}} \int_x \left[\frac{1}{a^m} \xi_m(x) e^{im\phi} \partial_x q + \text{h.c.} \right]. \quad (\text{II.14})$$

These two types of scattering correspond to “clean” and “dirty” current relaxations. Intuitively, the vortex operator $e^{im\phi} \sim (\psi_R \psi_L^\dagger)^m$, where $m \in \mathbb{N}^+$. The momentum mismatch \bar{k}_m in (II.13) equals

$$\bar{k}_m = mk_F - p_m G \in [0, 2\pi), \quad (\text{II.15})$$

where G is the reciprocal lattice vector (assuming an underlying lattice). For commensurate fillings, there is an integer p such that $\bar{k}_m = 0$. $\xi_m(x)$ is a quenched random variable with Gaussian statistics:

$$\overline{\xi_m(x)} = 0, \quad \overline{\xi_m(x) \xi_{m'}^*(x')} = D_m \delta_{mm'} \delta(x - x'), \quad (\text{II.16})$$

where the overline represents the disorder average.

H_m^U and H_m^{dis} are scattering processes between m left-moving and m right-moving fermions. The leading processes occur at $m = 1$. $e^{im\phi}$ has scaling dimension $\Delta_m(K) = m^2 K$. For commensurate fillings, λ_m^U has (leading) beta function $\beta_m^U = (2 - (\Delta_m + 1)) \lambda_m^U = (1 - \Delta_m) \lambda_m^U$. (The “1” in $(\Delta_m + 1)$ arises from the spatial derivative on the dimensionless phonon field q .) Thus, λ_m^U is relevant for $\Delta_m < 1$; this occurs for any repulsive interaction ($K < 1$) at $m = 1$. We use the convention that a positive beta function corresponds to a relevant operator and a negative beta function corresponds to an irrelevant operator. For incommensurate fillings, the exponential term $e^{i\bar{k}_m x}$ renders λ_m^U effectively zero at long distances. Upon performing the usual (replicated) disorder average [13], the variance D_m has (leading) beta function $\beta_m^{\text{dis}} = (3 - 2(\Delta_m + 1)) D_m = (1 - 2\Delta_m) D_m$. Thus, the disorder-mediated scattering is irrelevant for $\Delta_m > 1/2$ and relevant for $\Delta_m < 1/2$. In our calculation, we *assume* both types of scattering processes are weak. Given the above analysis, this occurs with umklapp scattering at incommensurate fillings or with disorder-mediated scattering for $1/2 < K \leq 1$.

III. TRANSPORT AT LOW AND HIGH TEMPERATURES

A. Memory Matrix

The memory matrix $\hat{\mathcal{M}}(\omega)$ is a convenient way to encode the transport properties of any system. Its definition and relation to the electrical and thermal conductivities proceed as follows:

$$\hat{\mathcal{M}}(\omega) = \sum_m (\hat{\mathcal{M}}_m^U(\omega) + \hat{\mathcal{M}}_m^{\text{dis}}(\omega)), \quad (\text{III.1})$$

where the contribution of each scattering process is

$$(\hat{\mathcal{M}}_m^U)^{\mathcal{Q}\mathcal{Q}'} = \frac{1}{L} \frac{\langle F_{m,\mathcal{Q}}^U; F_{m,\mathcal{Q}'}^U \rangle_\omega - \langle F_{m,\mathcal{Q}}^U; F_{m,\mathcal{Q}'}^U \rangle_{\omega=0}}{i\omega}, \quad (\text{III.2})$$

$$(\hat{\mathcal{M}}_m^{\text{dis}})^{\mathcal{Q}\mathcal{Q}'} = \frac{1}{L} \frac{\langle F_{m,\mathcal{Q}}^{\text{dis}}; F_{m,\mathcal{Q}'}^{\text{dis}} \rangle_\omega - \langle F_{m,\mathcal{Q}}^{\text{dis}}; F_{m,\mathcal{Q}'}^{\text{dis}} \rangle_{\omega=0}}{i\omega}. \quad (\text{III.3})$$

Here, $F_{\alpha,\mathcal{Q}}^U = i[H_\alpha^U, \mathcal{Q}]$, $F_{\alpha,\mathcal{Q}}^{\text{dis}} = \frac{i}{\sqrt{D_m}}[H_\alpha^{\text{dis}}, \mathcal{Q}]$, and the conserved current $\mathcal{Q} \in \{J_D, J_e, J_T\}$. $\langle F_{m,\mathcal{Q}}^U; F_{m,\mathcal{Q}'}^U \rangle_\omega$ and $\langle F_{m,\mathcal{Q}}^{\text{dis}}; F_{m,\mathcal{Q}'}^{\text{dis}} \rangle_\omega$ are finite-temperature retarded Green's functions, evaluated at real frequency ω . Notice that $\hat{\mathcal{M}}_m(\omega)$ has a zero eigenvalue for any current that commutes with H_m^U (or H_m^{dis}). The static susceptibility matrix $\hat{\chi}$ is the retarded finite-temperature Green's function:

$$\hat{\chi}_{\mathcal{Q}\mathcal{Q}'} = (\mathcal{Q}|\mathcal{Q}') \equiv \frac{1}{L} G_{\mathcal{Q}\mathcal{Q}'}(\omega = 0). \quad (\text{III.4})$$

The static susceptibility defines the overlap of two currents. Finite overlap between two currents implies that their transport is correlated.

The conductivity matrix $\hat{\sigma}(\omega)$ is defined in terms of the memory matrix $\hat{\mathcal{M}}$ and static susceptibility $\hat{\chi}$:

$$\hat{\sigma}(\omega) = \hat{\chi}(\hat{\mathcal{M}}(\omega) - i\omega\hat{\chi})^{-1}\hat{\chi}. \quad (\text{III.5})$$

Intuitively, the memory matrix formalism first computes the resistivity and then inverts to get the conductivity. This order of computation is especially useful for our system, with infinite conductivity in the decoupled limit. The electrical conductivity $\sigma(\omega)$ is the submatrix $\hat{\sigma}(\omega)_{J_e J_e}$ and the thermal conductivity $\kappa(\omega) = \hat{\sigma}(\omega)_{J_T J_T}/T$. The thermoelectric conductivity $\tilde{\alpha}$ is always 0 in our work, since there is no overlap between J_e and J_T or J_D , i.e., $(J_e|J_T) = (J_e|J_D) = 0$. We get the dc electrical σ and thermal κ conductivities by taking $\omega \rightarrow 0$.

B. Umklapp scattering

In this section, we sketch the calculation of the conductivity matrix $\hat{\sigma}$ (III.5) due to umklapp scattering (II.13). To begin, the static susceptibilities (III.4):

$$\hat{\chi}_{J_e J_e} = \frac{e^2 v_e K}{32}, \quad (\text{III.6})$$

$$16\hat{\chi}_{J_T J_T} = \hat{\chi}_{J_D J_D} = 4\hat{\chi}_{J_D J_T} = 4\hat{\chi}_{J_T J_D} = \frac{\pi^3 v_e T^2}{339}, \quad (\text{III.7})$$

$$\hat{\chi}_{J_e J_T} = \hat{\chi}_{J_T J_e} = \hat{\chi}_{J_e J_D} = \hat{\chi}_{J_D J_e} = 0. \quad (\text{III.8})$$

The calculation of these Green's functions is standard, with all details relegated to Appendix A. Note that the static susceptibilities are independent of the particular relaxation mechanism and so these susceptibilities will also be used in the next section when we consider disorder scattering.

We next turn to the memory matrix $(\hat{\mathcal{M}}_m^U)^{\mathcal{Q}\mathcal{Q}'}$, where $\mathcal{Q} \in \{J_D, J_e, J_T\}$. According to (III.2) and using results in Appendix B, we need the retarded Green's functions:

$$\begin{aligned} \frac{1}{L} \langle F_{m, J_e}^U; F_{m, J_e}^U \rangle_\omega &\propto \frac{1}{L} \int_{t, x, y} e^{i\omega t} \left\langle \frac{\sin(\bar{k}_m x + m\phi(x, t)) \sin(\bar{k}_m y + m\phi(y, 0))}{a^m} \right\rangle \\ &\times \langle \partial_x q(x, t) \partial_y q(y, 0) \rangle, \\ &= \frac{1}{4L} \int_{t, x, y} e^{i\omega t} \left[e^{i\bar{k}_m(x-y)} \left\langle \frac{e^{im\phi(x, t)} e^{-im\phi(y, 0)}}{a^m} \right\rangle \right. \\ &\left. + e^{-i\bar{k}_m(x-y)} \left\langle \frac{e^{-im\phi(x, t)} e^{im\phi(y, 0)}}{a^m} \right\rangle \right] \times \langle \partial_x q(x, t) \partial_y q(y, 0) \rangle, \end{aligned} \quad (\text{III.9})$$

$$\begin{aligned} \frac{1}{L} \langle F_{m, \mathcal{P}}^U; F_{m, \mathcal{P}'}^U \rangle_\omega &\propto \frac{1}{L} \int_{t, x, y} e^{i\omega t} \left\langle \frac{\cos(\bar{k}_m x + m\phi(x, t)) \cos(\bar{k}_m y + m\phi(y, 0))}{a^m} \right\rangle \\ &\times \langle \partial_x^2 q(x, t) \partial_y^2 q(y, 0) \rangle, \\ &= \frac{1}{4L} \int_{t, x, y} e^{i\omega t} \left[e^{i\bar{k}_m(x-y)} \left\langle \frac{e^{im\phi(x, t)} e^{-im\phi(y, 0)}}{a^m} \right\rangle \right. \\ &\left. + e^{-i\bar{k}_m(x-y)} \left\langle \frac{e^{-im\phi(x, t)} e^{im\phi(y, 0)}}{a^m} \right\rangle \right] \times \langle \partial_x^2 q(x, t) \partial_y^2 q(y, 0) \rangle, \end{aligned} \quad (\text{III.10})$$

where $\mathcal{P}, \mathcal{P}' \in \{J_T, J_D\}$. We have simplified the above expressions by leaving out constant proportionality factors. The real-space two-point functions of fermions/phonons $g_{e/p}(x, t)$ are:

$$g_e(x_-, t) \equiv \left\langle \frac{e^{\pm im\phi(x, t)} e^{\mp im\phi(y, 0)}}{a^m} \right\rangle = e^{C_e(x_-, t)}, \quad (\text{III.11})$$

where

$$C_e(x, t) \equiv \Delta_m(K) \ln \left[\frac{\pi a T / v_e}{\sinh(\pi T(x - v_e t + ia) / v_e)} \right] + \Delta_m(K) \ln \left[\frac{\pi a T / v_e}{\sinh(\pi T(x + v_e t - ia) / v_e)} \right], \quad (\text{III.12})$$

and

$$g_p(x_-, t) \equiv \langle \partial_x q(x, t) \partial_y q(y, 0) \rangle = \frac{(\pi a T / v_p)^2}{\sinh(\pi T(x_- - v_p t + ia) / v_p) \sinh(\pi T(x_- + v_p t - ia) / v_p)}. \quad (\text{III.13})$$

Recall that $\Delta_m(K) = m^2 K$. We are presenting the calculation for general $m \geq 1$ and K ; we will later specialize to the leading $m = 1$ case and repulsive interactions $K < 1$.

The spatial integrals above can be written as

$$\int dx dy = \frac{1}{2} \int dx_+ dx_-, \quad (\text{III.14})$$

where $x_{\pm} = x \pm y$. Because all the correlation functions are functions of x_- only, the integral over x_+ produces a factor of L that cancels the L^{-1} factor in the definition of memory matrix. We will drop all “-” subscripts in subsequent equations.

We now seek to evaluate the $\langle F; F \rangle_{\omega}$; these are essentially Fourier transforms of products of correlation functions. The memory matrix $(\hat{\mathcal{M}}_m^U)^{\mathcal{Q}\mathcal{Q}'}$ for umklapp scattering can be written as

$$(\hat{\mathcal{M}}_m^U)^{J_e J_e} = A_{m, J_e}^U A_{m, J_e}^U \frac{G_1(\bar{k}_m, \omega) - G_1(\bar{k}_m, \omega = 0)}{i\omega} + (\bar{k}_m \rightarrow -\bar{k}_m), \quad (\text{III.15})$$

$$(\hat{\mathcal{M}}_m^U)^{\mathcal{P}\mathcal{P}'} = A_{m, \mathcal{P}}^U A_{m, \mathcal{P}'}^U \frac{\tilde{G}_1(\bar{k}_m, \omega) - \tilde{G}_1(\bar{k}_m, \omega = 0)}{i\omega} + (\bar{k}_m \rightarrow -\bar{k}_m), \quad (\text{III.16})$$

where the constant coefficients $A_{m, \mathcal{P}}^i$ are given in Appendix B and the G -functions are defined as

$$G_1(k, \omega) = \int_{x, t} e^{i(\omega t - kx)} g_e(x, t) g_p(x, t), \quad (\text{III.17})$$

$$\tilde{G}_1(k, \omega) = - \int_{x, t} e^{i(\omega t - kx)} g_e(x, t) (\partial_x^2 g_p(x, t)), \quad (\text{III.18})$$

$$G_0^{e/p}(k, \omega) = \int_{x, t} e^{i(\omega t - kx)} g_{e/p}(x, t). \quad (\text{III.19})$$

The abbreviation $f \equiv \int_{x, t} \int_{-\infty}^{\infty} dt \int_{-\infty}^{\infty} dx$ and $\mathcal{P}, \mathcal{P}' \in \{J_D, J_T\}$. The dc limit is obtained by taking $\omega \rightarrow 0$. In this limit, the memory matrix is identical to the first derivative of the correlation

function:

$$\lim_{\omega \rightarrow 0} (\hat{\mathcal{M}}_m^U)^{J_e J_e} = A_{m, J_e}^U A_{m, J_e}^U (-i \partial_\omega G_1(\bar{k}_m, \omega)) \Big|_{\omega=0} + (\bar{k}_m \rightarrow -\bar{k}_m), \quad (\text{III.20})$$

$$\lim_{\omega \rightarrow 0} (\hat{\mathcal{M}}_m^U)^{\mathcal{P} \mathcal{P}'} = A_{m, \mathcal{P}}^U A_{m, \mathcal{P}'}^U (-i \partial_\omega \tilde{G}_1(\bar{k}_m, \omega)) \Big|_{\omega=0} + (\bar{k}_m \rightarrow -\bar{k}_m). \quad (\text{III.21})$$

We use the Fourier transforms of $g_e(x, t)$ and $g_p(x, t)$ in Eq.(III.19) to write $G_1(\bar{k}_m, \omega)$ in a form that is amenable to taking both the low and high temperature limits:

$$G_1(\bar{k}_m, \omega) = \int_{x, t} e^{i(\omega t - \bar{k}_m x)} g_e(x, t) g_p(x, t) = \frac{1}{(2\pi)^2} \int_{k, \omega_1} G_0^e(k, \omega_1) G_0^p(-k + \bar{k}_m, \omega - \omega_1). \quad (\text{III.22})$$

The integrals over momentum k and frequency ω should receive a correction in the high temperature regime that depends on the Debye cutoff Θ_D . We replace the integrals over momentum and frequency as

$$\int_{-\infty}^{\infty} dk \rightarrow \int_{-k_D}^{k_D} dk, \quad \int_{-\infty}^{\infty} d\omega_1 \rightarrow \int_{-\omega_D}^{\omega_D} d\omega_1, \quad (\text{III.23})$$

and then change variables to make the integrals dimensionless:

$$\int_{-k_D}^{k_D} dk \rightarrow \int_{-\Theta_D/T}^{\Theta_D/T} \frac{dk}{T}, \quad \int_{-\omega_D}^{\omega_D} d\omega_1 \rightarrow \int_{-\Theta_D/T}^{\Theta_D/T} \frac{d\omega_1}{T}. \quad (\text{III.24})$$

The Debye temperature $\Theta_D \equiv k_D v_p / 2\pi = \omega_D / 2\pi$.

In the low-temperature regime ($T \ll \Theta_D$), the integrals over momentum and frequency are given (to leading approximation) by the integrals with cutoff $\Theta_D \rightarrow \infty$. As a result, the low-temperature correlation function $G_1^<(\bar{k}_m, \omega)$ is

$$G_1^<(\bar{k}_m, \omega) \approx \left(\frac{2\pi T a}{v_e}\right)^{2\Delta_m} \left(\frac{\pi T a}{v_p}\right)^2 \frac{2v_p}{\pi^2 T^2} \int_0^\infty \frac{e^{-(\Delta_m - iq_-)s_+}}{\sinh(s_+)} \int_0^\infty \frac{e^{-(\Delta_m - iq_+)s_-}}{\sinh(s_-)}. \quad (\text{III.25})$$

Here, $s_\pm = \frac{\pi T}{v_p}(x \pm v_p t)$ and $q_\pm = (\omega \pm \bar{k}_m v_p) / 2\pi T$. The integrals are evaluated using the saddle point approximation [12]. The memory matrix that results is

$$\lim_{\omega \rightarrow 0} (\hat{\mathcal{M}}_m^U)^{J_e J_e} < \approx A_{m, J_e}^U A_{m, J_e}^U \left(\frac{2\pi T a}{v_e}\right)^{2\Delta_m} \left(\frac{\pi^2 a^2}{v_p T}\right) e^{-|\bar{k}_m v_p| / 2T}. \quad (\text{III.26})$$

Notice the exponential suppression as $T \rightarrow 0$ for incommensurate fillings $\bar{k}_m \neq 0$.

In the high temperature regime ($T \gg \Theta_D$), the integrals over momentum and frequency in Eq. (III.22) reduce (to leading approximation) to evaluating the integrands at $k = \omega_1 = 0$. We find

$$G_1^>(\bar{k}_m, \omega) = \frac{1}{(2\pi)^2} \int_{k, \omega_1} G_0^e(k, \omega_1) G_0^p(-k + \bar{k}_m, \omega - \omega_1) \approx \frac{k_D \omega_D}{\pi^2} G_0^e(0, 0) G_0^p(\bar{k}_m, \omega), \quad (\text{III.27})$$

where

$$G_0^e(0, 0) = \left(\frac{2\pi T a}{v_e}\right)^{2\Delta_m - 2} \frac{a^2}{2v_e} [B(\frac{\Delta_m}{2}, 1 - \Delta_m)]^2, \quad (\text{III.28})$$

$$G_0^p(\bar{k}_m, \omega) = \frac{a^2}{2v_p} \int_0^\infty \frac{e^{iq_- s_+}}{\sinh(s_+)} \int_0^\infty \frac{e^{iq_+ s_-}}{\sinh(s_-)}. \quad (\text{III.29})$$

Hence, the dc memory matrix at high temperatures is (to first approximation)

$$\lim_{\omega \rightarrow 0} (\hat{\mathcal{M}}_m^U)_{>}^{J_e J_e} \approx A_{m, J_e}^U A_{m, J_e}^U \left(\frac{2\pi T a}{v_e}\right)^{2\Delta_m} \frac{a^2 k_D v_e \omega_D}{16 v_p T^3} B^2\left(\frac{\Delta_m}{2}, 1 - \Delta_m\right) e^{-|\bar{k}_m v_p|/2T}. \quad (\text{III.30})$$

Above, $B(\alpha, \beta) = \Gamma(\alpha)\Gamma(\beta)/\Gamma(\alpha + \beta)$ is the beta function.

Putting it all together, the dc electrical conductivity is found to be

$$\sigma \propto \begin{cases} T^{1-2\Delta_m} e^{|\bar{k}_m v_p|/2T}, & T \ll \Theta_D, \\ T^{3-2\Delta_m} e^{|\bar{k}_m v_p|/2T}, & T \gg \Theta_D. \end{cases} \quad (\text{III.31})$$

Now consider the memory matrix for thermal transport. At low temperatures, the memory matrix is given by

$$\lim_{\omega \rightarrow 0} (\hat{\mathcal{M}}_m^U)_{<}^{\mathcal{P}\mathcal{P}'} = A_{m, \mathcal{P}}^U A_{m, \mathcal{P}'}^U \left(\frac{2\pi T a}{v_e}\right)^{2\Delta_m} \frac{\pi^4 T a^2}{v_p^3} e^{-|\bar{k}_m v_p|/2T}. \quad (\text{III.32})$$

To extract the high temperature behavior, we use the Fourier transform trick again, writing:

$$\tilde{G}_1(\bar{k}_m, \omega) = \frac{1}{(2\pi)^2} \int_{k, \omega_1} (k + \bar{k}_m)^2 G_0^e(-k, \omega_1) G_0^p(k + \bar{k}_m, \omega - \omega_1). \quad (\text{III.33})$$

The correlation function at high temperatures is (to leading approximation)

$$\tilde{G}_1^>(\bar{k}_m, \omega) \approx G_0^e(0, 0) \times \begin{cases} k_D \omega_D (\Delta k_\alpha)^2 G_0^p(\bar{k}_m, \omega) / \pi^2, & \bar{k}_m \neq 0, \\ k_D^3 \omega_D G_0^p(0, \omega) / 3\pi^2, & \bar{k}_m = 0. \end{cases} \quad (\text{III.34})$$

Thus, we have

$$\lim_{\omega \rightarrow 0} (\hat{\mathcal{M}}_m^U)_{>}^{\mathcal{P}\mathcal{P}'} = A_{m, \mathcal{P}}^U A_{m, \mathcal{P}'}^U \left(\frac{2\pi T a}{v_e}\right)^{2\Delta_m} \frac{a^2 k_D v_e \omega_D}{16\pi^2 v_p T^3} \times \begin{cases} (\bar{k}_m)^2 e^{-|\bar{k}_m v_p|/2T}, & \bar{k}_m \neq 0, \\ k_D^2 / 3, & \bar{k}_m = 0. \end{cases} \quad (\text{III.35})$$

Thus, we find the dc thermal conductivity:

$$\kappa \propto \begin{cases} T^{2-2\Delta_m} e^{|\bar{k}_m v_p|/2T}, & T \ll \Theta_D, \\ T^{-2\Delta_m} e^{|\bar{k}_m v_p|/2T}, & T \gg \Theta_D. \end{cases} \quad (\text{III.36})$$

The Lorentz ratio is

$$\mathcal{L} = \frac{\kappa}{T\sigma} \propto \begin{cases} \text{constant} & , T \ll \Theta_D, \\ T^2 & , T \gg \Theta_D. \end{cases} \quad (\text{III.37})$$

C. Regularizing the free fermion point

The following analysis will be used when we discuss the crossover temperature. Fix $m = 1$ and denote $\Delta \equiv \Delta_1(K) = K$, in order to focus on the leading scattering process.

Notice that $B(\frac{\Delta}{2}, 1 - \Delta)$, which occurs in (III.30) and (III.34), diverges when $\Delta \rightarrow 1$. This is a UV divergence that occurs at the free fermion point $K = 1$:

$$B\left(\frac{\Delta}{2}, 1 - \Delta\right) = \frac{1}{1 - \Delta} + \log(4) + \mathcal{O}(1 - \Delta). \quad (\text{III.38})$$

This divergence can be regularized by a nonzero short-distance cutoff on G_0^e in (III.19). This provides a cutoff-dependent definition of $B(\frac{\Delta}{2}, 1 - \Delta)$, and therefore the high temperature memory matrix elements (III.30) and (III.34), when $\Delta = 1$. Instead of imposing a finite short-distance cutoff, we replace $B(\frac{\Delta}{2}, 1 - \Delta) \rightarrow B_{\text{reg}}(\frac{\Delta}{2}, 1 - \Delta)$, with the ‘‘regularized beta function’’ defined via the subtraction:

$$B_{\text{reg}}\left(\frac{\Delta}{2}, 1 - \Delta\right) \equiv B\left(\frac{\Delta}{2}, 1 - \Delta\right) - \frac{1}{1 - \Delta}. \quad (\text{III.39})$$

This subtraction scheme corresponds to a specific short-distance cutoff, which in turn defines the memory matrix element at the free fermion point. This allows the smooth evaluation of memory matrix elements both at and away from the free fermion point.

D. Disorder scattering

In this section, we present the conductivity matrix $\hat{\sigma}$ (III.5) due to disorder scattering (II.14). The detailed calculation is in Appendix C.

The dc electrical memory matrix is

$$\lim_{\omega \rightarrow 0} (\hat{\mathcal{M}}_m^{\text{dis}})^{J_e J_e} \approx A_{m, J_e}^{\text{dis}} A_{m, J_e}^{\text{dis}} \left(\frac{2\pi T a}{v_e}\right)^{2\Delta_m + 2} \frac{\pi v_e^2}{v_p^2 T^2}, \quad (\text{III.40})$$

$$\lim_{\omega \rightarrow 0} (\hat{\mathcal{M}}_m^{\text{dis}})^{J_e J_e} \approx A_{m, J_e}^{\text{dis}} A_{m, J_e}^{\text{dis}} \left(\frac{2\pi T a}{v_e}\right)^{2\Delta_m + 2} \frac{k_D^2 v_e^3 \omega_D}{64\pi^5 v_p T^5} B_{\text{reg}}^2\left(\frac{\Delta_m}{2}, 1 - \Delta_m\right), \quad (\text{III.41})$$

where we have used the ‘‘regularized beta function’’ given in (III.39). Thus, the dc electrical conductivity σ is

$$\sigma \propto \begin{cases} T^{-2\Delta_m}, & T \ll \Theta_D, \\ T^{3-2\Delta_m}, & T \gg \Theta_D. \end{cases} \quad (\text{III.42})$$

For $\mathcal{P}, \mathcal{P}' \in \{J_T, J_D\}$, the dc thermal memory matrix below and above the Debye temperature is found to be

$$\lim_{\omega \rightarrow 0} (\hat{\mathcal{M}}_m^{\text{dis}})^{\mathcal{P}\mathcal{P}'} < \approx A_{m,\mathcal{P}}^{\text{dis}} A_{m,\mathcal{P}'}^{\text{dis}} \left(\frac{2\pi T a}{v_e} \right)^{2\Delta_m+2} \frac{v_e^2 \pi^3}{v_p^4}, \quad (\text{III.43})$$

$$\lim_{\omega \rightarrow 0} (\hat{\mathcal{M}}_m^{\text{dis}})^{\mathcal{P}\mathcal{P}'} > \approx A_{m,\mathcal{P}}^{\text{dis}} A_{m,\mathcal{P}'}^{\text{dis}} \left(\frac{2\pi T a}{v_e} \right)^{2\Delta_m+2} \frac{k_D^4 v_e^3 \omega_D}{192\pi^5 v_p T^5} B_{\text{reg}}^2 \left(\frac{\Delta_m}{2}, 1 - \Delta_m \right). \quad (\text{III.44})$$

The corresponding dc thermal conductivity κ scales as

$$\kappa \propto \begin{cases} T^{1-2\Delta_m}, & T \ll \Theta_D, \\ T^{6-2\Delta_m}, & T \gg \Theta_D. \end{cases} \quad (\text{III.45})$$

The Lorentz ratio is

$$\mathcal{L} = \frac{\kappa}{T\sigma} \propto \begin{cases} \text{constant}, & T \ll \Theta_D \\ T^2, & T \gg \Theta_D. \end{cases} \quad (\text{III.46})$$

The Lorentz ratio for disorder scattering is also non-constant, similar to what we found for the umklapp scattering.

IV. CROSSOVER TEMPERATURE

In the previous section we presented the conductivity matrix for umklapp and disorder scattering processes (II.13) and (II.14), for general m . We now specialize to the leading scattering term $m = 1$, corresponding to the phonon-mediated scattering between a single left and right moving fermion. Below we denote $\Delta_1 \equiv \Delta = K$.

The crossover temperature $T_0^{i,j}$ is where the low and high temperature transport asymptotics coincide (see Fig. 1):

$$\lim_{\omega \rightarrow 0} (\hat{\mathcal{M}}_m^i)^{\mathcal{Q}\mathcal{Q}'} < = \lim_{\omega \rightarrow 0} (\hat{\mathcal{M}}_m^i)^{\mathcal{Q}\mathcal{Q}'} >. \quad (\text{IV.1})$$

Here, the superscripts on $T_0^{i,j}$ indicate the scattering mechanism $i \in \{U, \text{dis}\}$ and different types of transport $j \in \{e, \text{th}\}$. For example, $T_0^{U,e}$ is the crossover temperature for the electrical resistivity due to umklapp scattering.

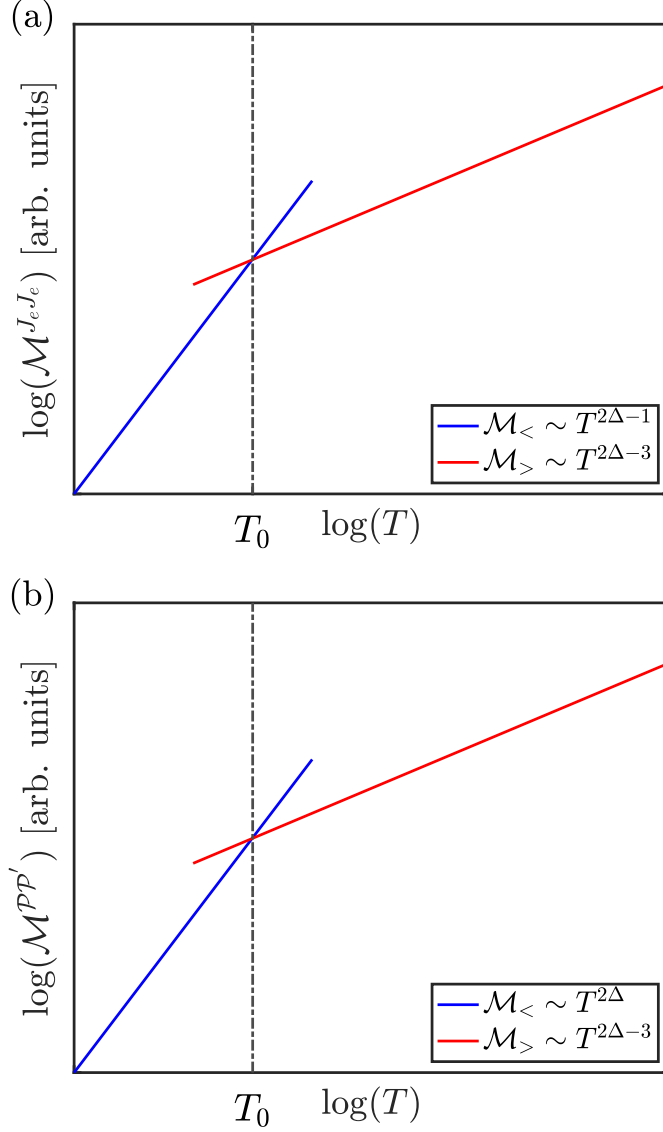


FIG. 1: Low and high temperature asymptotics of the memory matrix \mathcal{M} with intervening crossover temperature T_0 in the (a) clean (unklapp-dominated) and (b) dirty (disorder-dominated) limits. Blue (Red) lines are low (high)-temperature asymptotics of the memory matrices, and $\mathcal{P}, \mathcal{P}' \in \{J_T, J_D\}$.

Solving (IV.1) for $T_0^{i,j}$, we find

$$T_0^{i,j} = T_*^{i,j} f^{2/n}(\Delta), \quad (\text{IV.2})$$

where $n = 2$ when $(i, j) = (U, e)$, $n = 3$ when $(i, j) = (\text{dis}, e)$, $n = 4$ when $(i, j) = (U, \text{th})$, $n = 5$ when $(i, j) = (\text{dis}, \text{th})$, and

$$f(\Delta) = \frac{1}{\log(4)} B_{\text{reg}}\left(\frac{\Delta}{2}, 1 - \Delta\right). \quad (\text{IV.3})$$

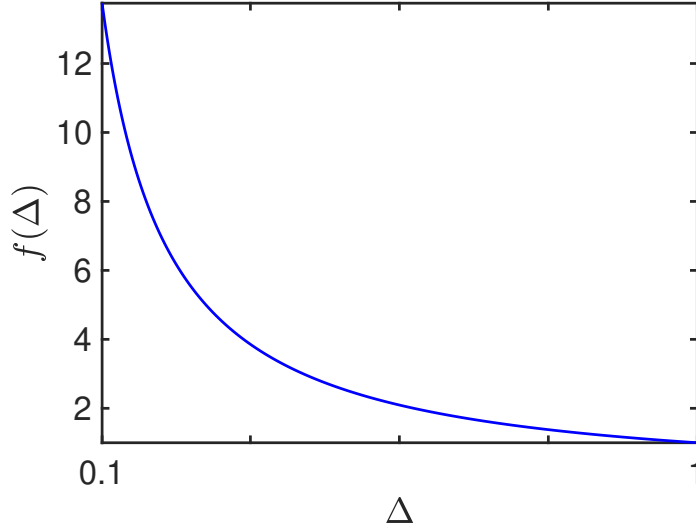


FIG. 2: Enhancement factor: $f(\Delta)$ determines in (IV.2) how the crossover temperature varies with interaction strength, here implicitly measured by Δ . Non-interacting fermions correspond to $\Delta = 1$; repulsive interactions occur for $\Delta < 1$.

$f(\Delta)$ is the enhancement factor that shows how the crossover temperature depends on interactions. Recall the regularized beta function B_{reg} in (III.39). The constant coefficient $T_*^{i,\mathcal{Q}}$ is the value of the crossover temperature at the free fermion point $\Delta = K = 1$. We find:

$$T_*^{U,e} = \left[\frac{1}{2\pi^2} \frac{v_e}{v_p} \log(4) \right]^{1/2} \Theta_D, \quad (\text{IV.4})$$

$$T_*^{U,\text{th}} = \left[\frac{2}{\pi^2} \frac{v_e}{v_p} \log(4) \right]^{1/4} \times \begin{cases} \Theta_D/3^{1/4}, & \bar{k}_1 = 0, \\ (\bar{k}_1 v_p \Theta_D / 2\pi)^{1/2}, & \bar{k}_1 \neq 0, \end{cases} \quad (\text{IV.5})$$

$$T_*^{\text{dis},e} = \left[\frac{1}{8\pi^3} \frac{v_e}{v_p} \log(4) \right]^{1/3} \Theta_D, \quad (\text{IV.6})$$

$$T_*^{\text{dis},\text{th}} = \left[\frac{1}{6\pi^3} \frac{v_e}{v_p} \log(4) \right]^{1/5} \Theta_D. \quad (\text{IV.7})$$

The Debye temperature $\Theta_D \equiv k_D v_p / 2\pi = \omega_D / 2\pi$.

We interpret (IV.2) as showing how the crossover temperature varies with the strength of the repulsive interaction $K < 1$, relative to its value at the noninteracting fixed point. We plot the universal function $f(\Delta)$ in Fig. 2. Notice that $f(\Delta)$ varies by about an order of magnitude as the strength of the repulsive interaction is increased (i.e., as K is decreased). The span of this variation is greater for the umklapp scattering than the disorder scattering and greater for electrical conductivity relative to the thermal conductivity. This universal dependence of the crossover temperature is the primary result of this paper.

The electrical and thermal crossover temperatures both depend on the same universal function $f(\Delta)$. This can be expressed succinctly by considering the following ratios:

$$\frac{(T_0^{U,\text{th}})^4}{(T_0^{U,e})^2} = \begin{cases} 4\Theta_D^2/3, & \bar{k}_1 = 0, \\ (\bar{k}_1 v_p/\pi)^2, & \bar{k}_1 \neq 0, \end{cases} \quad (\text{IV.8})$$

$$\frac{(T_0^{\text{dis,th}})^5}{(T_0^{\text{dis,e}})^3} = \frac{4}{3}\Theta_D^2. \quad (\text{IV.9})$$

Knowledge of the crossover temperature of the electrical conductivity determines the corresponding crossover temperature of the thermal conductivity. This assumes the same relaxation mechanism is operative for both conserved quantities.

V. CONCLUSION

We studied charge and heat transport in an interacting Luttinger liquid coupled to acoustic phonons using the memory matrix formalism. By explicitly incorporating the Debye cutoff in electron-phonon correlation functions, we computed the dc conductivities across low and high temperature regimes in both clean (umklapp-dominated) and dirty (disorder-dominated) limits.

Our central result is that the crossover temperature T_0 between quantum and classical transport regimes is enhanced by repulsive electronic correlations: $T_0 \sim \Theta_D \times f(K)$, where Θ_D is the Debye temperature and the universal function $f(K)$ increases by an order of magnitude as strength of repulsive electron-electron interactions is increased—this occurs as the Luttinger parameter K varies from the free fermion point $K = 1$ to $K = 0$. This interaction-dependent enhancement provides a possible explanation for the persistence of fixed power-law resistivity across wide temperatures in strongly correlated systems: the low-temperature scattering regime is extended to higher temperatures, with the would-be high-temperature regime rendered unobservable. While the crossover temperatures independently depend on the universal function $f(K)$, ratios of the electrical and thermal crossover temperatures are interaction-independent in our model. Our results suggest that strong correlations don't just modify transport exponents—they also alter the temperature scales separating different scattering regimes.

While our one-dimensional model neglects spin degrees of freedom and vertex corrections, the mechanism we identify—interaction-enhanced crossover scales—may be general to strongly correlated systems. It may be interesting to consider the crossover temperature in more general one-dimensional Luttinger liquids with more channels, which feature additional symmetries and robust low-temperature phases [14, 15]. The extension to higher dimensions is of great interest: a particularly interesting and tractable model may be that of [7].

ACKNOWLEDGMENTS

We thank Sankar Das Sarma, Hart Goldman, Steve Kivelson, Chao-Jung Lee, Sri Raghu, and Jörg Schmalian for helpful discussions. This work was supported by the U.S. Department of Energy, Office of Science, Office of Basic Energy Sciences, under Award No. DE-SC0020007. M.M. acknowledges the kind hospitality of the Kavli Institute for Theoretical Physics, which is supported in part by the National Science Foundation under Grants No. NSF PHY-1748958 and PHY-2309135, during the completion of this work.

Appendix A: Static Susceptibilities

The static susceptibility matrix $\hat{\chi}_{\mathcal{Q}\mathcal{Q}'} = G_{\mathcal{Q}\mathcal{Q}'}^R(\omega = 0)/L$, where \mathcal{Q} is a conserved current. We start with the electrical current,

$$J_e = \frac{ev_e K}{4} \int_x \Pi(x). \quad (\text{A.1})$$

In general, the retarded Green's function $G_{\mathcal{Q}\mathcal{Q}'}^R(\omega)$ can be obtained by Wick rotating the corresponding Euclidean Green's function $G_{\mathcal{Q}\mathcal{Q}'}^E(i\omega_E \rightarrow \omega + i\delta)$, where ω_E is the Euclidean frequency. The Euclidean Green's function is (setting $\delta \rightarrow 0$)

$$\hat{\chi}_{J_e J_e} \equiv \frac{1}{L} \lim_{\omega_E \rightarrow 0} \int_{\tau} e^{i\omega_E \tau} \langle J_e(\tau) J_e(0) \rangle = \left(\frac{ev_e K}{4}\right)^2 \lim_{\omega_E \rightarrow 0} \frac{1}{L} \int_{\tau, x, y} e^{i\omega_E \tau} \langle \Pi(x, \tau) \Pi(y, 0) \rangle, \quad (\text{A.2})$$

where the Euclidean time $\tau \in [0, 1/T]$, and $\langle \dots \rangle$ stands for thermal average. We have the famous result in conformal field theory

$$\langle \Pi(x, \tau) \Pi(y, 0) \rangle = \frac{1}{64\pi K} \left[\frac{(\pi T/v_e)^2}{\sinh^2(\pi T(x - y - iv_e \tau)/v_e)} + \frac{(\pi T/v_e)^2}{\sinh^2(\pi T(x - y + iv_e \tau)/v_e)} \right]. \quad (\text{A.3})$$

We generalize the integral by replacing the exponents from $2 \rightarrow 2h$, $h \in \mathbb{N}^+$. By performing the contour integral, we have the general expression

$$\frac{1}{L} \int_{\tau, x, y} e^{i\omega_E \tau} \frac{(\pi T/v_i)^{2h}}{\sinh^{2h}(\pi T(x - y + ipv_i \tau)/v_i)} = \frac{2\pi}{\omega_E} \frac{(2\pi T/v_i)^{2h-1}}{(2h-1)!} \prod_{j=1}^{2h-1} \left(\frac{\omega_E}{2\pi T} + h - j \right), \quad p = \pm. \quad (\text{A.4})$$

As a result, we have

$$\hat{\chi}_{J_e J_e} = \frac{e^2 v_e K}{32}. \quad (\text{A.5})$$

On the other hand, the thermal current J_T and momentum deviation from the Fermi surface J_D are given by

$$J_T = -\frac{v_e^2}{4} \int_x \Pi(\partial_x \phi) - v_p^2 \int d^3 x P(\partial_x q), \quad (\text{A.6})$$

$$J_D = -v_e^2 \int_x \Pi(\partial_x \phi) - v_e^2 \int d^3 x P(\partial_x q). \quad (\text{A.7})$$

The static susceptibility,

$$\begin{aligned} \hat{\chi}_{J_T J_T} &\equiv \frac{1}{V} \lim_{\omega_E \rightarrow 0} \int_{\tau} e^{i\omega_E \tau} \langle J_T(\tau) J_T(0) \rangle \\ &\approx \frac{v_e^4}{16} \times \lim_{\omega_E \rightarrow 0} \frac{1}{L} \int_{\tau, x, y} e^{i\omega_E \tau} \langle \Pi(x, \tau) \Pi(y, 0) \rangle \langle \partial_x \phi(x, \tau) \partial_y \phi(y, 0) \rangle \\ &= \frac{\pi^3 v_e T^2}{1356}. \end{aligned} \quad (\text{A.8})$$

Similarly, we have

$$\hat{\chi}_{J_D J_D} = \hat{\chi}_{J_D J_T} \approx \frac{\pi^3 v_e T^2}{339}, \quad (\text{A.9})$$

$$\hat{\chi}_{J_e J_T} = \hat{\chi}_{J_T J_e} = \hat{\chi}_{J_e J_D} = \hat{\chi}_{J_D J_e} = 0. \quad (\text{A.10})$$

Appendix B: Evaluation of $F_{m,\mathcal{Q}}^i$

In the limit $v_p \ll v_e$, $F_{m,\mathcal{Q}}^U = i[H_m^U, \mathcal{Q}]$, and $F_{m,\mathcal{Q}}^{\text{dis}} = \frac{i}{\sqrt{D_m}}[H_m^{\text{dis}}, \mathcal{Q}]$ are:

$$F_{m,J_e}^U = A_{m,J_e}^U \int_x \frac{1}{a^m} \sin(\bar{k}_m x + m\phi) (\partial_x q), \quad (\text{B.1})$$

$$F_{m,\mathcal{P}}^U \approx A_{m,\mathcal{P}}^U \int_x \frac{1}{a^m} \cos(\bar{k}_m x + m\phi) (\partial_x^2 q), \quad (\text{B.2})$$

$$F_{m,J_e}^{\text{dis}} = \frac{A_{m,J_e}^{\text{dis}}}{\sqrt{D_m}} \left[\int_x \frac{1}{a^m} \xi_m(x) e^{im\phi} (\partial_x q) - h.c. \right], \quad (\text{B.3})$$

$$F_{m,\mathcal{P}}^{\text{dis}} \approx \frac{A_{m,\mathcal{P}}^{\text{dis}}}{\sqrt{D_m}} \left[\int_x \frac{1}{a^m} \xi_m e^{im\phi} (\partial_x^2 q) + h.c. \right], \quad (\text{B.4})$$

where $\mathcal{P} \in \{J_T, J_D\}$. The coefficients $A_{m,\mathcal{Q}}^i$ are

$$A_{m,J_e}^U = \frac{i\pi e v_e K}{2}, \quad (\text{B.5})$$

$$A_{m,J_D}^U = 4v_p^2, \quad (\text{B.6})$$

$$A_{m,J_T}^U = 2v_e^2 + 2v_p^2, \quad (\text{B.7})$$

$$A_{m,J_e}^{\text{dis}} = -\frac{e v_e K m}{4}, \quad (\text{B.8})$$

$$A_{m,J_D}^{\text{dis}} = v_e^2, \quad (\text{B.9})$$

$$A_{m,J_T}^{\text{dis}} = v_p^2. \quad (\text{B.10})$$

The approximation indicated by “ \approx ” is leading for $v_p \ll v_e$.

Appendix C: Disorder Scattering Memory Matrix Details

The retarded Green's function $\frac{1}{L} \langle F_{m,J_e}^{\text{dis}}, F_{m,J_e}^{\text{dis}} \rangle_\omega$ is

$$\frac{1}{L} \langle F_{m,J_e}^{\text{dis}}, F_{m,J_e}^{\text{dis}} \rangle_\omega = \frac{A_{m,J_e}^{\text{dis}} A_{m,J_e}^{\text{dis}}}{LD_m} \int_{x,y,t} e^{i\omega t} g_e(x-y, t) g_p(x-y, t) [\xi_m(x) \xi_m^*(y) + \xi_m^*(x) \xi_m(y)]. \quad (\text{C.1})$$

We perform an integration by parts and drop all boundary terms to obtain $\frac{1}{L}\langle F_{m,\mathcal{P}}^{\text{dis}}; F_{m,\mathcal{P}'}^{\text{dis}} \rangle_\omega$ for $\mathcal{P}, \mathcal{P}' \in \{J_T, J_D\}$:

$$\frac{1}{L}\langle F_{m,\mathcal{P}}^{\text{dis}}, F_{m,\mathcal{P}'}^{\text{dis}} \rangle_\omega = -\frac{A_{m,\mathcal{P}}^{\text{dis}}A_{m,\mathcal{P}'}^{\text{dis}}}{LD_m} \int_{x,y,t} e^{i\omega t} g_e(x,t) (\partial_x^2 g_p(x,t)) [\xi_m(x)\xi_m^*(y) + \xi_m^*(x)\xi_m(y)]. \quad (\text{C.2})$$

After disorder averaging $\overline{\xi_m(x)\xi_m^*(y)} = D_m\delta(x-y)$, we obtain

$$\frac{1}{L}\langle F_{m,J_e}^{\text{dis}}, F_{m,J_e}^{\text{dis}} \rangle_\omega = 2A_{m,J_e}^{\text{dis}}A_{m,J_e}^{\text{dis}}G_2(\omega), \quad (\text{C.3})$$

$$\frac{1}{L}\langle F_{m,\mathcal{P}}^{\text{dis}}, F_{m,\mathcal{P}'}^{\text{dis}} \rangle_\omega = 2A_{m,\mathcal{P}}^{\text{dis}}A_{m,\mathcal{P}'}^{\text{dis}}\tilde{G}_2(\omega), \quad (\text{C.4})$$

The memory matrix $(\hat{\mathcal{M}}_m^{\text{dis}})^{\mathcal{P}\mathcal{P}'}$ is

$$(\hat{\mathcal{M}}_m^{\text{dis}})^{J_eJ_e} = 2A_{m,J_e}^{\text{dis}}A_{m,J_e}^{\text{dis}}\frac{G_2(\omega) - G_2(\omega=0)}{i\omega}, \quad (\text{C.5})$$

$$(\hat{\mathcal{M}}_m^{\text{dis}})^{\mathcal{P}\mathcal{P}'} = 2A_{m,\mathcal{P}}^{\text{dis}}A_{m,\mathcal{P}'}^{\text{dis}}\frac{\tilde{G}_2(\omega) - \tilde{G}_2(\omega=0)}{i\omega}, \quad (\text{C.6})$$

where $G_2(\omega)$ and $\tilde{G}_2(\omega)$ are

$$G_2(\omega) = \int_{x,t} e^{i\omega t} g_e(x,t)g_p(x,t)\delta(x), \quad (\text{C.7})$$

$$\tilde{G}_2(\omega) = -\int_{x,t} e^{i\omega t} g_e(x,t)(\partial_x^2 g_p(x,t))\delta(x). \quad (\text{C.8})$$

We take the dc limit $\omega \rightarrow 0$:

$$\lim_{\omega \rightarrow 0} (\hat{\mathcal{M}}_m^{\text{dis}})^{J_eJ_e} = 2A_{m,J_e}^{\text{dis}}A_{m,J_e}^{\text{dis}}(-i\partial_\omega G_2(\omega))\Big|_{\omega=0}, \quad (\text{C.9})$$

$$\lim_{\omega \rightarrow 0} (\hat{\mathcal{M}}_m^{\text{dis}})^{\mathcal{P}\mathcal{P}'} = 2A_{m,\mathcal{P}}^{\text{dis}}A_{m,\mathcal{P}'}^{\text{dis}}(-i\partial_\omega \tilde{G}_2(\omega))\Big|_{\omega=0}. \quad (\text{C.10})$$

To include the Debye cut-off, we apply the Fourier transform trick described in the main text, writing

$$G_2(\omega) = \int_{x,t} e^{i\omega t} g_e(x,t)g_p(x,t)\delta(x) = \frac{1}{8\pi^3} \int_{k_1,k_2,\omega_1} G_0^e(k_1,\omega_1)G_0^p(k_2,\omega-\omega_1) \quad (\text{C.11})$$

$$\tilde{G}_2(\omega) = -\int_{x,t} e^{i\omega t} g_e(x,t)(\partial_x^2 g_p(x,t))\delta(x) = \frac{1}{8\pi^3} \int_{k_1,k_2,\omega_1} k_2^2 G_0^e(k_1,\omega_1)G_0^p(k_2,\omega-\omega_1). \quad (\text{C.12})$$

The dc electrical memory matrices below and above the Debye temperature are found to be

$$\lim_{\omega \rightarrow 0} (\hat{\mathcal{M}}_m^{\text{dis}})^{J_e J_e} < \approx A_{m, J_e}^{\text{dis}} A_{m, J_e}^{\text{dis}} \left(\frac{2\pi T a}{v_e} \right)^{2\Delta_m + 2} \frac{\pi v_e^2}{v_p^2 T^2}, \quad (\text{C.13})$$

$$\lim_{\omega \rightarrow 0} (\hat{\mathcal{M}}_m^{\text{dis}})^{J_e J_e} > \approx A_{m, J_e}^{\text{dis}} A_{m, J_e}^{\text{dis}} \left(\frac{2\pi T a}{v_e} \right)^{2\Delta_m + 2} \frac{k_D^2 v_e^3 \omega_D}{64\pi^5 v_p T^5} B^2 \left(\frac{\Delta_m}{2}, 1 - \Delta_m \right). \quad (\text{C.14})$$

Hence, the dc electrical conductivity σ is given by

$$\sigma \propto \begin{cases} T^{-2\Delta_m}, & T \ll \Theta_D, \\ T^{3-2\Delta_m}, & T \gg \Theta_D. \end{cases} \quad (\text{C.15})$$

The dc thermal memory matrices at low and high temperatures are given by

$$\lim_{\omega \rightarrow 0} (\hat{\mathcal{M}}_m^{\text{dis}})^{\mathcal{P}\mathcal{P}'} < \approx A_{m, \mathcal{P}}^{\text{dis}} A_{m, \mathcal{P}'}^{\text{dis}} \left(\frac{2\pi T a}{v_e} \right)^{2\Delta_m + 2} \frac{v_e^2 \pi^3}{v_p^4}, \quad (\text{C.16})$$

$$\lim_{\omega \rightarrow 0} (\hat{\mathcal{M}}_m^{\text{dis}})^{\mathcal{P}\mathcal{P}'} > \approx A_{m, \mathcal{P}}^{\text{dis}} A_{m, \mathcal{P}'}^{\text{dis}} \left(\frac{2\pi T a}{v_e} \right)^{2\Delta_m + 2} \frac{k_D^4 v_e^3 \omega_D}{192\pi^5 v_p T^5} B^2 \left(\frac{\Delta_m}{2}, 1 - \Delta_m \right). \quad (\text{C.17})$$

The dc thermal conductivity κ is

$$\kappa \propto \begin{cases} T^{1-2\Delta_m}, & T \ll \Theta_D, \\ T^{6-2\Delta_m}, & T \gg \Theta_D. \end{cases} \quad (\text{C.18})$$

- [1] E. W. Carlson, V. J. Emery, S. A. Kivelson, and D. Orgad, Concepts in high temperature superconductivity, in Superconductivity: Conventional and Unconventional Superconductors, edited by K. H. Bennemann and J. B. Ketterson (Springer Berlin Heidelberg, Berlin, Heidelberg, 2008) pp. 1225–1348.
- [2] C. M. Varma, Colloquium: Linear in temperature resistivity and associated mysteries including high temperature superconductivity, *Rev. Mod. Phys.* **92**, 031001 (2020).
- [3] Y. Cao, D. Rodan-Legrain, O. Rubies-Bigorda, J. M. Park, K. Watanabe, T. Taniguchi, and P. Jarillo-Herrero, Strange metal in magic-angle graphene with near planckian dissipation, *Phys. Rev. Lett.* **124**, 076801 (2020).
- [4] S. A. Hartnoll and A. P. Mackenzie, Colloquium: Planckian dissipation in metals, *Rev. Mod. Phys.* **94**, 041002 (2022).
- [5] C. M. Varma, P. B. Littlewood, S. Schmitt-Rink, E. Abrahams, and A. E. Ruckenstein, Phenomenology of the normal state of cu-o high-temperature superconductors, *Phys. Rev. Lett.* **63**, 1996 (1989).
- [6] D. Chowdhury, A. Georges, O. Parcollet, and S. Sachdev, Sachdev-ye-kitaev models and beyond: Window into non-fermi liquids, *Rev. Mod. Phys.* **94**, 035004 (2022).

- [7] N. Bashan, E. Tulipman, J. Schmalian, and E. Berg, Tunable Non-Fermi Liquid Phase from Coupling to Two-Level Systems, *Phys. Rev. Lett.* **132**, 236501 (2024), arXiv:2310.07768 [cond-mat.str-el].
- [8] S. Ahn and S. Das Sarma, Planckian properties of two-dimensional semiconductor systems, *Phys. Rev. B* **106**, 155427 (2022).
- [9] E. H. Hwang and S. Das Sarma, t -linear resistivity in dilute metals: A fermi liquid perspective, *Phys. Rev. B* **99**, 085105 (2019).
- [10] J. Zaanen, Planckian dissipation, minimal viscosity and the transport in cuprate strange metals, *SciPost Physics* **6**, 061 (2019).
- [11] J. Ziman, Electrons and Phonons: The Theory of Transport Phenomena in Solids, International series of monographs on physics (OUP Oxford, 2001).
- [12] E. Shimshoni, N. Andrei, and A. Rosch, Thermal conductivity of spin- $\frac{1}{2}$ chains, *Phys. Rev. B* **68**, 104401 (2003).
- [13] T. Giamarchi, Quantum Physics in One Dimension (Oxford University Press, 2003).
- [14] E. Plamadeala, M. Mulligan, and C. Nayak, Perfect metal phases of one-dimensional and anisotropic higher-dimensional systems, *Phys. Rev. B* **90**, 241101 (2014).
- [15] E. Plamadeala, M. Mulligan, and C. Nayak, Transport in a one-dimensional hyperconductor, *Phys. Rev. B* **93**, 125142 (2016).